Journal of Applied Mechanics Vol.10, pp.723-732 (August 2007) JSCE

A Non-Linear k-ε Model to Predict the Spatial Change of Turbulent Structures in Large Scale Vortices

Md. Shahjahan Ali *, Takashi Hosoda **, Ichiro Kimura***

* PhD Student, Department of Urban Management, Kyoto University (606-8501, Kyoto)
** Professor, Department of Urban Management, Kyoto University (606-8501, Kyoto)
***Department of Civil and Environmental Engineering, Matsue National College of Technology, (690-8518, Matsue)

Flows with large scale vortices are often observed in many natural, geophysical as well as anthropogenic activities. In this study, the Stuart vortices having both the singular points (the vortex and saddle points) are considered to study the basic turbulent properties. Using a realizable non-linear k-ε model, the approximate solutions are derived and numerical simulations are carried out. Using the approximate solution, the values of model constants are tuned considering the predictability of turbulent structures at the vortex center. The numerical results prove the effectiveness of the approximate approach, and reveals that the model with the estimated constants is applicable to simulate large scale vortices. The spatial changes in the topological structures of turbulent energy and turbulent stresses are found compatible with the previous experimental results.

Key Words: *Stuart vortex, non-linear k - ε model, RANS, realizability conditions*

1. Introduction

The presence of large scale vortices in a flow field plays an important role in the intermittent character of turbulence. The horizontal vortex at the interface of main channel and flood plain in a compound channel is a practical example of that. In a compound channel, because of the velocity gradient between main channel and flood plain, large-scale vortices are generated with the vertical axis at the interface. The vortex formation causes momentum transfer in the lateral direction from the main channel to the flood plains, results in the decrease of channel conveyance and increase of the flow resistance. Since the turbulent characteristics of this type of flows are highly non-linear, the standard k-ε model cannot produce such flows satisfactorily because of its isotropic assumption of eddy viscosity; on the other hand, the empirical functions in a non-linear k- ε model plays an important role to generate the large scale vortices by accounting the anisotropic turbulent behavior. Therefore, a non-linear k- ε model is thought to be a superior tool for predicting such complex flows. The superiority of non-linear k- ε model over standard one is described in our previous paper considering approximate solutions for some basic turbulent flows such as non-swirl and swirl jet (Ali et. al.)[1]. However, the applicability of this model to large scale vortices is still to examine.

The non-linear $k-\varepsilon$ model is a generalized eddy viscosity model, where additional non-linear terms of mean strain rate are added. In other words, it is a two equation model where two differential equations are solved for k and ε, and the Reynolds stresses are determined from non-linear algebraic equations by generalizing the eddy viscosity model. Yoshizawa[2] introduced such non-linear relation to Reynolds stresses to admit the anisotropy. Generally, in $k-\varepsilon$ model, the value of the coefficient of eddy viscosity (c_μ) is assumed constant throughout the turbulent flow field. This constant value of c_μ over predicts the eddy viscosity for the flow field having large rate of strain and rotation. If the strain is sufficiently large, the model may produce negative normal stresses. Thus, in the present study, the coefficient of eddy viscosity (c_μ) is considered as a function of strain (S) and rotation (Ω) parameters. Considering the Reynolds stresses as a non-linear polynomial function of mean velocity gradient, such functional form for the coefficient of eddy viscosity was firstly introduced by Pope[3], but that was

limited to two dimensional flows. Gatski and Spezille[4] further extended it and proposed a new functional form applicable for three dimensional flows. Recently, Kimura and Hosoda[5] verified the modified $k-\varepsilon$ model with the non-linear anisotropy term. They assumed a functional form of c_μ similar to Pope[3], and examined the realizability conditions for different types of 2D basic flow patterns.

In this study, the Stuart vortices having both the singular points (the vortex and saddle points) are considered to study the basic turbulent properties. The work presented in this paper can be classified into twofold. In the first part, a heuristic solution is derived for turbulent characteristics of Stuart vortices, to investigate the necessary conditions for a non-linear k- ε model applicable to large-scale vortices. In the second part of the paper, numerical simulations are carried out to support the approximate solution.

Previous experimental and numerical investigations[6] showed that the structures of turbulent normal stresses at vortex point are elliptical in shape; on the other hand, the turbulent shear stresses show hyperbolic profile. By tuning the model constants in the approximate solution, it is observed that the structures of turbulent stresses are changed with the values of constants. The set of model constants that generates the actual structures of turbulent profiles, is considered to be satisfied the necessary conditions for unsteady-RANS applicable to large-scale vortices. The realizability conditions are also derived for a plane shear layer to estimate the constraints for the coefficients of eddy viscosity. In the second part, using the model constants estimated by approximate solution, the numerical simulation is carried out to determine the turbulent characteristics of Stuart vortices, and the qualitative structures are compared with approximate solutions as well as with previous experimental results[6]. The spatial changes in the topological structures of turbulent energy and turbulent stresses are also explained.

2. Non-Linear k - ε Model

2.1 Basic equations

The basic equations in a k - ε model for an unsteady incompressible flow are as follows.
Continuity equation:

$$\frac{\partial U_i}{\partial x_i} = 0 \tag{1}$$

Momentum equation:

$$\frac{\partial U_i}{\partial t} + \frac{\partial U_j U_i}{\partial x_j} = g_i - \frac{1}{\rho}\frac{\partial P}{\partial x_i} + \frac{\partial}{\partial x_j}\left(-\overline{u_i u_j}\right) + \nu\frac{\partial^2 U_i}{\partial x_j^2} \tag{2}$$

k - equation:

$$\frac{\partial k}{\partial t} + \frac{\partial k U_j}{\partial x_j} = -\overline{u_i u_j}\frac{\partial U_i}{\partial x_j} + \frac{\partial}{\partial x_j}\left\{\left(\frac{\nu_t}{\sigma_k} + \nu\right)\frac{\partial k}{\partial x_j}\right\} - \varepsilon \tag{3}$$

ε - equation:

$$\frac{\partial \varepsilon}{\partial t} + \frac{\partial \varepsilon U_j}{\partial x_j} = -c_{\varepsilon 1}\frac{\varepsilon}{k}\overline{u_i u_j}\frac{\partial U_i}{\partial x_j} + \frac{\partial}{\partial x_j}\left\{\left(\frac{\nu_t}{\sigma_\varepsilon} + \nu\right)\frac{\partial \varepsilon}{\partial x_j}\right\} - c_{\varepsilon 2}\frac{\varepsilon^2}{k} \tag{4}$$

where, x_i : the spatial coordinates, U_i and u_i : the average and turbulent velocities respectively in x_i direction, P : the pressure, ρ : the density of fluid, ν : the molecular kinematic viscosity, k : the averaged turbulent energy, ε : the averaged turbulent energy dissipation rate, ν_t : the eddy viscosity, σ_k, σ_ε , $c_{\varepsilon 1}$, $c_{\varepsilon 2}$: the model constants (σ_k= 1.0, σ_ε= 1.3, $c_{\varepsilon 1}$ = 1.44 and $c_{\varepsilon 2}$ = 1.92 are used)[7].

2.2 Constitutive equations

In the standard $k-\varepsilon$ model, the Reynolds stress tensor $-\overline{u_i u_j}$ is solved by linear constitutive equations derived from Boussinesq eddy viscosity concept, which does not take into account the anisotropy effect.

$$-\overline{u_i u_j} = \nu_t S_{ij} - \frac{2}{3}k\delta_{ij}, \quad S_{ij} = \frac{\partial U_i}{\partial x_j} + \frac{\partial U_j}{\partial x_i} \tag{5}$$

Here, ν_t is determined from the dimensional consideration of k and ε, and is approximated by

$$\nu_t = c_\mu \frac{k^2}{\varepsilon} \quad . \tag{6}$$

Including the non-linear anisotropy term in the Reynolds stress equation introduced by Yoshizawa[2], the constitutive equations can be expressed in the following forms

$$-\overline{u_i u_j} = \nu_t S_{ij} - \frac{2}{3}k\delta_{ij} - \frac{k}{\varepsilon}\nu_t \sum_{\beta=1}^{3} c_\beta \left(S_{\beta ij} - \frac{1}{3}S_{\beta\alpha\alpha}\delta_{ij}\right) \tag{7}$$

Here, c_β is the coefficient of non-linear quadratic term; and $S_{\beta ij}$ are defined as :

$$S_{1ij} = \frac{\partial U_i}{\partial x_\gamma}\frac{\partial U_j}{\partial x_\gamma}, \quad S_{2ij} = \frac{1}{2}\left(\frac{\partial U_\gamma}{\partial x_i}\frac{\partial U_j}{\partial x_\gamma} + \frac{\partial U_\gamma}{\partial x_j}\frac{\partial U_i}{\partial x_\gamma}\right),$$

and $$S_{3ij} = \frac{\partial U_\gamma}{\partial x_i}\frac{\partial U_\gamma}{\partial x_j}. \tag{8}$$

It is known that the non-linear terms in equation (7) are equivalent to the following mathematical formulation[4, 5].

$$\alpha_1(S_{il}\Omega_{lj} + \Omega_{li}S_{jl}) + \alpha_2(S_{il}S_{lj} - \frac{1}{3}S_{km}S_{mk}\delta_{ij}) + \alpha_3(\Omega_{il}\Omega_{lj} - \frac{1}{3}\Omega_{km}\Omega_{mk}\delta_{ij}) \tag{9}$$

Where, the strain and rotation tensors are defined as

$$S_{ij} = \frac{\partial U_i}{\partial x_j} + \frac{\partial U_j}{\partial x_i}, \quad \Omega_{ij} = \frac{\partial U_i}{\partial x_j} - \frac{\partial U_j}{\partial x_i} \tag{10}$$

Comparing Eq. (9) with the non-linear terms of Eq. (7), the relations between the coefficients can be derived as

$$c_1 = -2\alpha_1 + \alpha_2 - \alpha_3, c_2 = 2(\alpha_2 + \alpha_3), c_3 = 2\alpha_1 + \alpha_2 - \alpha_3 \tag{11}$$

From this comparison, it is also inferred that the coefficient of eddy viscosity (c_μ) is a function of strain and rotation parameters. The strain parameter *(S)* and rotation parameter (Ω) are defined in Eq. (12), as used in the previous studies of Pope[3], and Gatski and Speziale[4].

$$S = \frac{k}{\varepsilon}\sqrt{\frac{1}{2}S_{ij}S_{ij}}, \quad \Omega = \frac{k}{\varepsilon}\sqrt{\frac{1}{2}\Omega_{ij}\Omega_{ij}} \tag{12}$$

In this study, the assumed form of c_μ is more generalized than previous one, which can be expressed as

$$c_\mu = \frac{c_{\mu o}\,(1 + c_{ns}S^2 + c_{n\Omega}\Omega^2)}{1 + c_{ds}S^2 + c_{d\Omega}\Omega^2 + c_{ds\Omega}S\Omega + c_{ds1}S^4 + c_{d\Omega 1}\Omega^4 + c_{ds\Omega 1}S^2\Omega^2} \tag{13}$$

Here, $c_{\mu 0}$, c_{ns}, $c_{n\Omega}$, c_{ds}, $c_{d\Omega}$, $c_{ds\Omega}$, c_{ds1}, $c_{d\Omega 1}$, and $c_{ds\Omega 1}$ are the model constants. The functional form assumed by Gatski and Speziale[13] can be obtained from the above equation simply neglecting some higher order terms i.e. substituting $c_{n\Omega}$, $c_{ds\Omega}$, c_{ds1}, and $c_{d\Omega 1}$ as zero. The more simplified functional form of c_μ, suggested by Pope[3] for two dimensional flows, can be obtained neglecting some more terms from the above equation.

Assuming a similar functional form for c_β, Kimura and Hosoda[5] compared the analytical results for diagonal components of the anisotropic tensor with that of experiments for simple shear flows. They showed that the assumed functional form for the coefficient of quadratic term c_β, gave better results instead of taking their constant values. In this analysis, the similar functional form is assumed for c_β.

$$c_\beta = c_{\beta o}\frac{1}{1 + m_{ds}S^2 + m_{d\Omega}\Omega^2} \tag{14}$$

where, m_{ds} and $m_{d\Omega}$ are the model constants.

3. Method of Solution

The work presented in this paper can be classified into two fold. In first part, a heuristic solution is derived for turbulent characteristics of Stuart vortices, to investigate the necessary conditions for a non-linear k- ε model applicable to large-scale vortices. In the second part of the paper, numerical simulations are conducted to support the approximate solution.

3.1 Approximate solution

The functional forms of k and ε distributions are assumed as a first approximation. Substituting the mathematical expressions of the assumed distributions into the non-linear $k - \varepsilon$ equations, a set of algebraic equations are derived considering the relation among the coefficients with respect to the same power of variables (x and y). Solving these simultaneous algebraic equations, the unknown coefficients in the assumed distributions are determined as the function of the non-linear $k - \varepsilon$ model constants. Approximate solutions for the distributions of turbulence characteristics such as distribution of turbulence intensities, turbulent shear stress, etc. are derived using the constitutive equations of the model.

Previous experimental and numerical simulations showed that the structures of turbulent normal stresses at vortex point are elliptical in shape; on the other hand, the turbulent shear stresses show hyperbolic profile. By tuning the model constants in the approximate solution, it is observed that the structures of turbulent stresses are changed with the values of constants. The set of model constants that generates the actual structures of turbulent profiles, is considered to be satisfied the necessary conditions for unsteady-RANS applicable to large-scale vortices. The realizability conditions are also derived for a plane shear layer to estimate the constraints for the coefficients of eddy viscosity.

3.2 Numerical simulation

Using the model constants estimated by approximate solution, the numerical simulation is carried out to determine the turbulent characteristics of Stuart vortices and the turbulent structures are compared with approximate solution.

The flow field of Stuart vortices is given as input to calculate the turbulent characteristics. The code solves the k, ε and constitutive equations discretized with the finite volume method and is based on a staggered grid system. The hybrid central upwind scheme is used for the k and ε equations. Time advancement is achieved by Adam-Bashforth scheme of second-order accuracy, in each equation. The equations are discretized as fully explicit forms and solved successively with the time increment step by step. The wall functions are employed as the wall boundary conditions for k and ε. Periodic boundary conditions are used in upstream and downstream ends of the flow domain.

4. Consideration of Realizability

4.1 Realizability inequalities

Realizability can be defined as the requirement of the non-negativity of turbulent normal stresses and Schwarz' inequality between any turbulent velocity correlations.[5] It is a basic physical and mathematical principle that the solution of any turbulence model equation should obey.[8] The realizability inequalities for 3D turbulent flows are:

$$\overline{u_i u_i} \geq 0 \tag{15a}$$

$$\overline{u_i u_i} \cdot \overline{u_j u_j} \geq \overline{u_i u_j}^2 \quad (i \neq j) \tag{15b}$$

$$\det \begin{bmatrix} \overline{u_1 u_1} & \overline{u_1 u_2} & \overline{u_1 u_3} \\ \overline{u_2 u_1} & \overline{u_2 u_2} & \overline{u_2 u_3} \\ \overline{u_3 u_1} & \overline{u_3 u_2} & \overline{u_3 u_3} \end{bmatrix} \geq 0 \tag{15c}$$

Einstein's summation rule is not applied in Eq. (15). In a two dimensional averaged flow, Eq. (15b) coincides with Eq. (15c). In this study, the restrictions on c_μ are derived from the mentioned realizability equations for simple shear flow. The functional forms for c_μ and c_β, expressed in Eqs. (13) and (14) respectively, are applied in this study.

4.2 Analysis of inequality for simple shear flow

Applying Eq. (15a) to plane shear layer, the following two equations are derived for the diagonal components of the Reynolds stress tensor (non-negativity condition)

$$\frac{\overline{u_1 u_1}}{k} = \frac{2}{3} + \frac{c_\mu (2c_1 - c_3)}{3} M^2 \geq 0 \tag{16a}$$

$$\frac{\overline{u_2 u_2}}{k} = \frac{2}{3} + \frac{c_\mu (2c_3 - c_1)}{3} M^2 \geq 0 \tag{16b}$$

Where, M = maximum (S,Ω); for plane shear layer, M=S=Ω. Applying Eq. (15b), the following inequality equation can be derived for Reynolds stress component, $\overline{u_1 u_2}$ (Schwarz' inequality condition).

$$c_\mu^2 \left\{ 9M^2 + (2c_1^2 + 2c_3^2 - 5c_1 c_3) M^4 \right\} - 2c_\mu (c_1 + c_3) M^2 - 4 \leq 0 \tag{16c}$$

Since the value of c_1 is positive and c_3 is negative, Eq. (16a) is satisfied regardless of M. Thus, the restrictions on c_μ, derived from Eqs. (16b) and (16c), are as follows:

$$c_\mu \leq \frac{2}{(c_1 - 2c_3) M^2} \tag{17}$$

$$c_\mu \leq \frac{(c_1 + c_3) M + \sqrt{(c_1 + c_3)^2 M^2 + 4\left\{9 + (2c_1^2 + 2c_3^2 - 5c_1 c_3) M^2\right\}}}{9M + (2c_1^2 + 2c_3^2 - 5c_1 c_3) M^3} \tag{18}$$

Following values, for the coefficients of functional forms of c_β, are proposed from our previous studies in flows around bluff bodies[5]:

c_{10} =0.40, c_{20} =0, and c_{30} = -0.13.

For plane shear layer, the realizability conditions [Eqs. (17) and (18)] as well as the proposed functional form of c_μ [Eq. (13)] are plotted in Fig. 1. The calculations are made with the following values of model constants.

$c_{\mu 0}$ = 0.09, c_{ns}+$c_{n\Omega}$= 0.0118, c_{ds}+$c_{d\Omega}$+$c_{ds\Omega}$ = 0.009, c_{ds1} +$c_{d\Omega 1}$+ $c_{ds\Omega 1}$= 0.00035, m_{ds} + $m_{d\Omega}$= 0.013 (19)

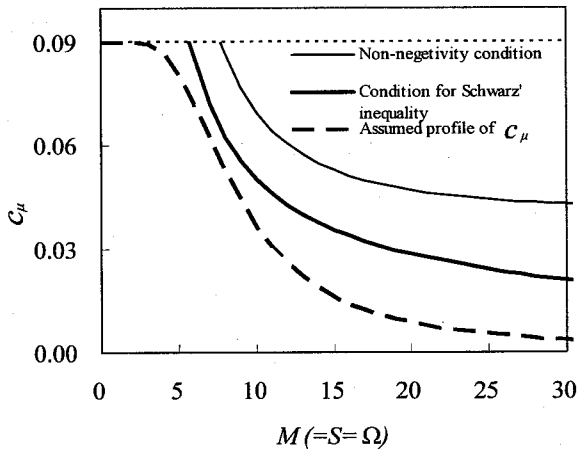

Fig.1 Relation between c_μ and M in a simple shear layer

These values of model constants are initially estimated based on the realizability conditions as derived in Eqs. (17) and (18). Using the estimated values, the approximate solutions are derived for Stuart vortices and the values of model constants are finally determined by tuning their values considering the predictability of turbulent structures. Eq.(19) shows the final values of constants obtained by such a trial and error method, and Fig. 1 confirms that the model obeys the realizability conditions with these values of constants.

In the log-law region, the assumed functional form of c_μ shows almost a constant value of 0.09. It can be noted that, instead of functional form, if a constant value of c_μ (=0.09) is used through out the turbulent flow field (shown as horizontal straight dotted line in the figure), it fails to satisfy the realizability conditions.

5. Turbulent Characteristics of Stuart Vortices

The Stuart vortices constitute a family of exact solutions of the Euler equations often used to model 2D mixing layers. The equation for stream function of the Stuart vortex can be expressed as follows:

$$\psi = \ln(\cosh y + A \cos x) \tag{20}$$

Here, $0 \geq A \geq -1$ is a constant and indicates the eccentricity of the elliptic streamline of vortex. If A=0, the

hyperbolic-tangent mixing layer is recovered, whereas for A=-1, we obtained a single row of co-rotating vortices, with circulation of -4π, periodically spaced along the x axis with period 2π. Fig. 2 shows the streamlines of Stuart vortices with various values of A. In this study, moderate eccentricity of A=- 0.5 is used to calculate the turbulent characteristics.

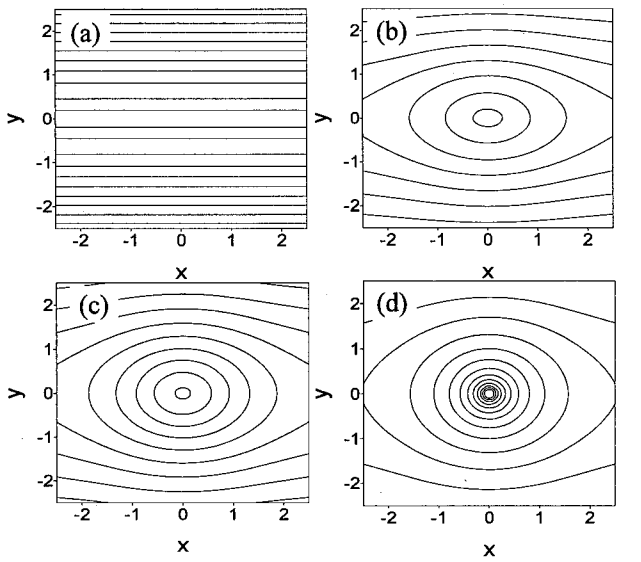

Fig.2 Contour of streamlines for Stuart vortex with (a) A=0 (b) A=-1/2 (c) A=-3/4 (d) A=-1.0

5.1 Derivation of approximate solutions

For the approximate analysis of Stuart vortices, the viscous shear stress is assumed much smaller than the turbulent shear stress[9]. Then the k and ε equations [Eqs. (3) and (4)] can be simplified for a steady two-dimensional flow in the following forms.

k - equation:

$$U_x\frac{\partial k}{\partial x}+U_y\frac{\partial k}{\partial y}=-\overline{u_xu_x}\frac{\partial U_x}{\partial x}-\overline{u_xu_y}\frac{\partial U_x}{\partial y}-\overline{u_yu_x}\frac{\partial U_y}{\partial x}$$
$$-\overline{u_yu_y}\frac{\partial U_y}{\partial y}+\frac{\partial}{\partial y}\left(\frac{\nu_t}{\sigma_k}\frac{\partial k}{\partial y}\right)+\frac{\partial}{\partial x}\left(\frac{\nu_t}{\sigma_k}\frac{\partial k}{\partial x}\right)-\varepsilon \qquad (21)$$

ε - equation:

$$U_x\frac{\partial \varepsilon}{\partial x}+U_y\frac{\partial \varepsilon}{\partial y}=c_{\varepsilon 1}\frac{\varepsilon}{k}\left[-\overline{u_xu_x}\frac{\partial U_x}{\partial x}-\overline{u_xu_y}\frac{\partial U_x}{\partial y}-\overline{u_yu_x}\frac{\partial U_y}{\partial x}\right.$$
$$\left.-\overline{u_yu_y}\frac{\partial U_y}{\partial y}\right]+\frac{\partial}{\partial y}\left(\frac{\nu_t}{\sigma_\varepsilon}\frac{\partial \varepsilon}{\partial y}\right)+\frac{\partial}{\partial x}\left(\frac{\nu_t}{\sigma_\varepsilon}\frac{\partial \varepsilon}{\partial x}\right)-c_{\varepsilon 2}\frac{\varepsilon^2}{k} \qquad (22)$$

The equation of Stuart vortices as expressed in Eq.(20) is expanded using Taylor function near the origin, and the approximated stream function for the vortex point is expressed as follows (eccentricity, A=- 0.5 is used)

$$\psi=\ln\left(1/2\right)+\frac{1}{2}x^2+y^2-\frac{1}{6}x^4-\frac{1}{2}x^2y^2-\frac{5}{12}y^4 \qquad (23)$$

The corresponding velocity field is approximated as

$$U_x=\frac{\partial \psi}{\partial y}=2y-x^2y-\frac{5}{3}y^3 \qquad (24)$$

$$U_y=-\frac{\partial \psi}{\partial x}=-x+xy^2+\frac{2}{3}x^3 \qquad (25)$$

The contour of streamlines for vortex point approximated by Taylor function near the origin (Eq. 22) is shown in Fig.3.

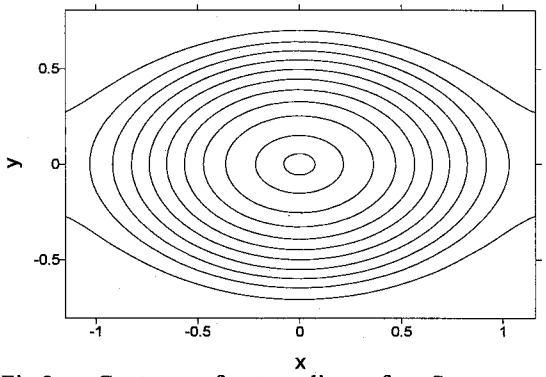

Fig.3 Contour of streamlines for Stuart vortex approximated by Taylor function near the origin

As first approximation, the following polynomial functional forms are assumed for the distributions of k and ε.

$$k=k_{00}+k_{01}x+k_{10}y++k_{02}x^2+k_{20}y^2+k_{11}xy \qquad (26)$$

$$\varepsilon=\varepsilon_{00}+\varepsilon_{01}x+\varepsilon_{10}y++\varepsilon_{02}x^2+\varepsilon_{20}y^2+\varepsilon_{11}xy \qquad (27)$$

Where, k_{00}, k_{01}, k_{10}, k_{02}, k_{20}, k_{11} are the unknown coefficients for k and ε_{00}, ε_{01}, ε_{10}, ε_{02}, ε_{20}, ε_{11} are that for ε distributions.

Substituting the assumed k and ε distributions, into $k-\varepsilon$ equations [Eqs. (21) and (22)], the following algebraic expressions are derived considering the relations of coefficients for the same power of variables (x, y) in each equation. To avoid complexity in solving a large number of equations, the higher order terms of k_{01}, k_{10}, k_{02}, k_{20}, k_{11}, ε_{01}, ε_{10}, ε_{02}, ε_{20} and ε_{11} are neglected to form a set of linear equations.

<u>k-equation</u>:

$$0:\ c_{\mu_0}k_{00}^2(1)_0-(2)_0+\frac{c_{\mu_0}}{\sigma_k}k_{00}^2\{2k_{02}+2k_{20}\}(1)_0=0 \qquad (28)$$

$$x:\ k_{10}=Ak_{01}+B\varepsilon_{01} \qquad (29)$$

$$y:\ 2k_{01}=Ak_{10}+B\varepsilon_{10} \qquad (30)$$

$$x^2:\ -k_{11}=Ak_{02}+B\varepsilon_{02}+C_5(k_{02}+k_{20})+C_1 \qquad (31)$$

$$y^2:\ 2k_{11}=Ak_{20}+B\varepsilon_{20}-C_6(k_{02}+k_{20})+C_2 \qquad (32)$$

$$xy:\ 4k_{02}-2k_{20}=Ak_{11}+B\varepsilon_{11} \qquad (33)$$

<u>ε -equation</u>:

$$0:\ c_{\varepsilon_1}c_{\mu_0}k_{00}^2\varepsilon_{00}^2(1)_0-c_{\varepsilon_2}\varepsilon_{00}^2(2)_0+\frac{c_{\mu_0}}{\sigma_\varepsilon}k_{00}^3\{2k_{02}+2k_{20}\}(1)_0=0 \qquad (34)$$

$$x:\ -\varepsilon_{10}=Ck_{01}+D\varepsilon_{01} \qquad (35)$$

$$y:\ 2\varepsilon_{01}=Ck_{10}+D\varepsilon_{10} \qquad (36)$$

$$x^2:\ -\varepsilon_{11}=Ck_{02}+D\varepsilon_{02}+C_7(\varepsilon_{02}+\varepsilon_{20})+C_3 \qquad (37)$$

$$y^2: \quad 2\varepsilon_{11} = Ck_{20} + D\varepsilon_{20} - C_8(\varepsilon_{02} + \varepsilon_{20}) + C_4 \qquad (38)$$

$$xy: \quad 4\varepsilon_{02} - 2\varepsilon_{20} = Ck_{11} + D\varepsilon_{11} \qquad (39)$$

Here,

$$A = \left[c_{\mu_0}\varepsilon_{00}k_{00}^3\{(1)_0(2m_{ds} + 18m_{d\Omega}) + (4)_0(2c_{ns} + 18c_{n\Omega})\}\right.$$
$$+ 2c_{\mu_0}\varepsilon_{00}k_{00}(1)_0(4)_0 - \varepsilon_{00}k_{00}(2)_0(2m_{ds} + 18m_{d\Omega})$$
$$\left. - \varepsilon_{00}k_{00}(4)_0 - \varepsilon_{00}k_{00}(4)_0\{\varepsilon_{00}^2(2c_{ds} + 6c_{ds\Omega} + 18c_{d\Omega}) + 4k_{00}^2(c_{ds1} + 9c_{ds\Omega 1} + 81c_{d\Omega 1})\}\right] / \{(2)_0(4)_0\}$$

$$B = \left[2c_{\mu_0}\varepsilon_{00}^2k_{00}^2\{(1)_0 + (4)_0\} + c_{\mu_0}k_{00}^2(1)_0(4)_0 - \{2(2)_0\varepsilon_{00}^2\right.$$
$$+ 4\varepsilon_{00}^4(4)_0 + \varepsilon_{00}^2k_{00}^2(4)_0(2c_{ds} + 6c_{ds\Omega} + 18c_{d\Omega})$$
$$\left. + (2)_0(4)_0\}\right] / \{(2)_0(4)_0\}$$

$$C = \left[c_{\mu_0}c_{\varepsilon_1}\varepsilon_{00}^2k_{00}^3\{(1)_0(2m_{ds} + 18m_{d\Omega}) + (4)_0(2c_{ns} + 18c_{n\Omega})\}\right.$$
$$+ 2c_{\mu_0}c_{\varepsilon_1}\varepsilon_{00}^2k_{00}(1)_0(4)_0 - c_{\varepsilon_2}\varepsilon_{00}^2k_{00}(2)_0(2m_{ds} + 18m_{d\Omega})$$
$$\left. - c_{\varepsilon_2}\varepsilon_{00}^2k_{00}(4)_0\{\varepsilon_{00}^2(2c_{ds} + 6c_{ds\Omega} + 18c_{d\Omega}) + 4k_{00}^2(c_{ds1} + 9c_{ds\Omega 1} + 81c_{d\Omega 1})\}\right] / \{(2)_0(4)_0k_{00}\}$$

$$D = \left[2c_{\mu_0}c_{\varepsilon_1}\varepsilon_{00}^3k_{00}^2\{(1)_0 + (4)_0\} + 2c_{\mu_0}c_{\varepsilon_1}\varepsilon_{00}k_{00}^2(1)_0(4)_0\right.$$
$$- c_{\varepsilon_2}\{2(2)_0\varepsilon_{00}^2 + 4\varepsilon_{00}^5(4)_0 + \varepsilon_{00}^3k_{00}^2(4)_0(2c_{ds} + 6c_{ds\Omega} + 18c_{d\Omega})$$
$$\left. + \varepsilon_{00}(2)_0(4)_0\}\right] / \{(2)_0(4)_0k_{00}\}$$

$$C_1 = \left[-\varepsilon_{00}k_{00}^2\{(2)_0(2m_{ds} - 18m_{d\Omega}) + \varepsilon_{00}^2(4)_0(2c_{ds} - 18c_{d\Omega})\}\right.$$
$$+ 2c_{\mu_0}\varepsilon_{00}k_{00}^2(1)_0(4)_0 + c_{\mu_0}\varepsilon_{00}k_{00}^4(1)_0(2m_{ds} - 18m_{d\Omega})$$
$$\left. + \varepsilon_{00}k_{00}^4(4)_0\{c_{\mu_0}(2c_{ns} - 18c_{n\Omega}) + 4(c_{ds1} - 81c_{d\Omega 1})\}\right] / \{(2)_0(4)_0\}$$

$$C_2 = \left[-\varepsilon_{00}k_{00}^2\{(2)_0(-8m_{ds} - 36m_{d\Omega}) - \varepsilon_{00}^2(4)_0(8c_{ds} + 36c_{d\Omega}\right.$$
$$\left. + 18c_{ds\Omega})\} - 8c_{\mu_0}\varepsilon_{00}k_{00}^2(1)_0(4)_0 + c_{\mu_0}\varepsilon_{00}k_{00}^4(1)_0(-8m_{ds}\right.$$
$$\left. - 36m_{d\Omega}) + \varepsilon_{00}k_{00}^4(4)_0\{c_{\mu_0}(-8c_{ns} - 36c_{n\Omega})\right.$$
$$\left. - 4(4c_{ds1} + 162c_{d\Omega 1} - 27c_{ds\Omega 1})\}\right] / \{(2)_0(4)_0\}$$

$$C_3 = \left[-c_{\varepsilon_2}\varepsilon_{00}^2k_{00}^2\{(2)_0(2m_{ds} - 18m_{d\Omega}) + \varepsilon_{00}^2(4)_0(2c_{ds}\right.$$
$$\left. - 18c_{ds\Omega})\} + 2c_{\mu_0}c_{\varepsilon_1}\varepsilon_{00}^2k_{00}^2(1)_0(4)_0 + c_{\mu_0}c_{\varepsilon_1}\varepsilon_{00}^2k_{00}^4(1)_0\right.$$
$$(2m_{ds} - 18m_{d\Omega}) + \varepsilon_{00}^2k_{00}^4(4)_0\{c_{\varepsilon_2}c_{\mu_0}(2c_{ns} - 18c_{n\Omega})$$
$$\left. + 4c_{\varepsilon 1}(c_{ds1} - 81c_{d\Omega 1})\}\right] / \{(2)_0(4)_0\}$$

$$C_4 = \left[-c_{\varepsilon_2}\varepsilon_{00}^2k_{00}^2\{(2)_0(-8m_{ds} - 36m_{d\Omega}) - \varepsilon_{00}^2(4)_0(8c_{ds}\right.$$
$$\left. + 36c_{d\Omega} + 18c_{ds\Omega})\} - 8c_{\mu_0}c_{\varepsilon_1}\varepsilon_{00}^2k_{00}^2(1)_0(4)_0 + c_{\mu_0}c_{\varepsilon_1}\varepsilon_{00}^2k_{00}^4(1)_0\right.$$
$$(-8m_{ds} - 36m_{d\Omega}) + \varepsilon_{00}^2k_{00}^4(4)_0\{c_{\mu_0}c_{\varepsilon_1}(-8c_{ns} - 36c_{n\Omega})$$
$$\left. - 4c_{\varepsilon_2}(4c_{ds1} + 162c_{d\Omega 1} - 27c_{ds\Omega 1})\}\right] / \{(2)_0(4)_0k_{00}\}$$

$$C_5 = \left[(2c_{\mu_0}/\sigma_k) - \varepsilon_{00}k_{00}^4\{(1)_0(2m_{ds} - 18m_{d\Omega})\right.$$
$$\left. + (4)_0(2c_{ns} - 18c_{n\Omega})\}\right] / \{(2)_0(4)_0\}$$

$$C_6 = \left[(2c_{\mu_0}/\sigma_k) - \varepsilon_{00}k_{00}^4\{(1)_0(8m_{ds} + 36m_{d\Omega})\right.$$
$$\left. + (4)_0(8c_{ns} + 36c_{n\Omega})\}\right] / \{(2)_0(4)_0\}$$

$$C_7 = \left[(2c_{\mu_0}/\sigma_\varepsilon) - \varepsilon_{00}k_{00}^4\{(1)_0(2m_{ds} - 18m_{d\Omega})\right.$$
$$\left. + (4)_0(2c_{ns} - 18c_{n\Omega})\}\right] / \{(2)_0(4)_0\}$$

$$C_8 = \left[(2c_{\mu_0}/\sigma_\varepsilon) - \varepsilon_{00}k_{00}^4\{(1)_0(8m_{ds} + 36m_{d\Omega})\right.$$
$$\left. + (4)_0(8c_{ns} + 36c_{n\Omega})\}\right] / \{(2)_0(4)_0\}$$

$$(1)_0 = \varepsilon_{00}^2 + c_{ns}k_{00}^2 + 9c_{n\Omega}k_{00}^2$$

$$(2)_0 = \varepsilon_{00}^2\left(\varepsilon_{00}^2 + c_{ds}k_{00}^2 + 3c_{ds\Omega}k_{00}^2 + 9c_{d\Omega}k_{00}^2\right)$$
$$+ k_{00}^4\left(c_{ds1} + c_{ds}k_{00}^2 + 9c_{ds\Omega 1} + 81c_{d\Omega 1}\right)$$

$$(4)_0 = \varepsilon_{00}^2 + m_{ds}k_{00}^2 + 9m_{d\Omega}k_{00}^2$$

Table1. Estimated values for the coefficients of c_μ and c_β

Model constants	Values of model constants	
	Run1	**Run2**
$c_{\mu 0}$	0.09	0.09
c_{ns}	0.005	0.01
$c_{n\Omega}$	0.0068	0.007
c_{ds}	0.008	0.008
$c_{d\Omega}$	0.004	0.004
$c_{ds\Omega}$	-0.003	-0.003
c_{ds1}	0.00005	0.00005
$c_{d\Omega 1}$	0.00005	0.00005
$c_{ds\Omega 1}$	0.00025	0.00025
m_{ds}	0.01	0.01
$m_{d\Omega}$	0.003	0.003

Solving the twelve equations from Eqs. (28) to (39), twelve unknowns are determined in terms of model constants. Then the distributions of turbulent intensities and shear stresses are derived by constitutive equations. Substituting the obtained values of unknown coefficients into assumed k and ε profiles in Eqs. (26) and (27), the profiles are inferred. It is reported that, the turbulent normal stresses, and hence k and ε profiles, show elliptical structure near the vortex point; on the other hand the turbulent shear stresses show hyperbolic profile. The values of model constants estimated from realizability considerations are tuned so that the turbulent structures become compatible with previous investigations[6]. The final values of model constants are tabulated in Table 1 (RUN-1). It can be noted that, the turbulent structure is changed with the change of the values of model constants. Among the numerous trials, one of the trial set of model constants are shows in RUN-2. The estimated values of c_{ns}, $c_{n\Omega}$ are 0.005 and 0.0068 respectively as shown in RUN-1. Keeping all other model constants as same as previous RUN-1, c_{ns} and $c_{n\Omega}$ are increased to 0.01 and 0.007 respectively in RUN-2 (the changed values are underlined in the table).

Although, the flow field is two-dimensional,

three-dimensional turbulent fields are calculated. Figs. 4 and 5 show the turbulent structures determined by approximate solution using the estimated model constants for RUN-1 and RUN-2 respectively. It is observed from Fig. 4 that, for RUN-1, turbulent kinetic energy (k) and its dissipation rate (ε) profiles [Figs. (a) and (b)] as well as the turbulent normal stresses in x, y and z direction expressed as u_1u_1, u_2u_2 and u_3u_3 respectively [Figs. (c), (d) and (e)] show elliptical structure; on the other hand the turbulent shear stress in xy plane (u_1u_2) show hyperbolic profile [Fig. (f)] near the center of vortex . On the other hand, if the model constants are changed to RUN-2, the same solution gives hyperbolic profiles for turbulent kinetic energy and turbulent normal stresses as shown in Fig. 5 (a), (c) and (d). Similar change is observed by the change of other model constant values. The turbulent structures are changed due to the change of c_μ distribution. The comparison of c_μ distribution in xy plane for Run-1 and Run-2 are shown in Fig. 6. Maximum difference is observed at the center of vortex, where the strain and rotation parameters have their maximum values.

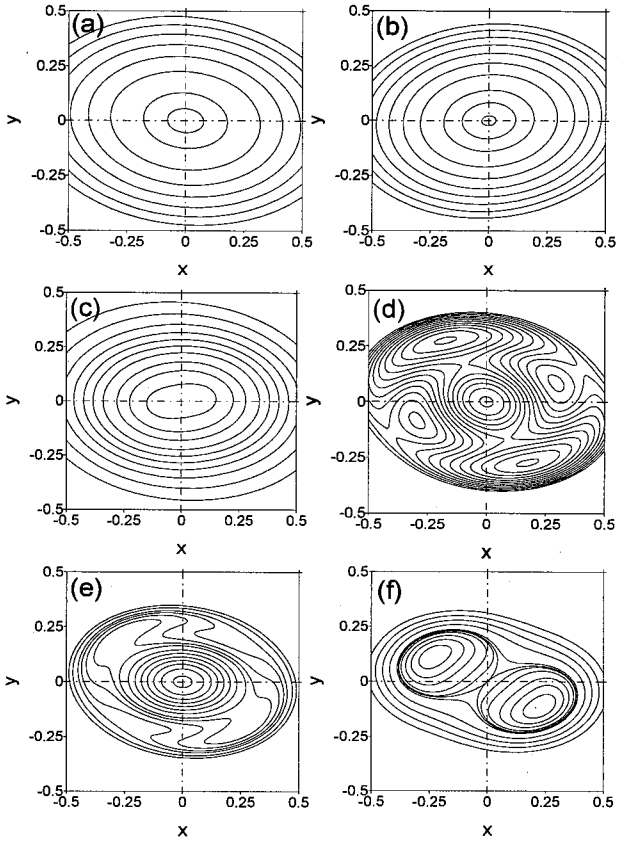

Fig.4 Turbulent structures by approximate solution for RUN-1: (a) turbulent kinetic energy, k (b) turbulent energy dissipation rate, ε (c) turbulent normal stress in x direction, $\overline{u_1u_1}$ (d) turbulent normal stress in y direction, $\overline{u_2u_2}$ (e) turbulent normal stress in z direction, $\overline{u_3u_3}$ (f) turbulent shear stress in xy plane, $\overline{u_1u_2}$.

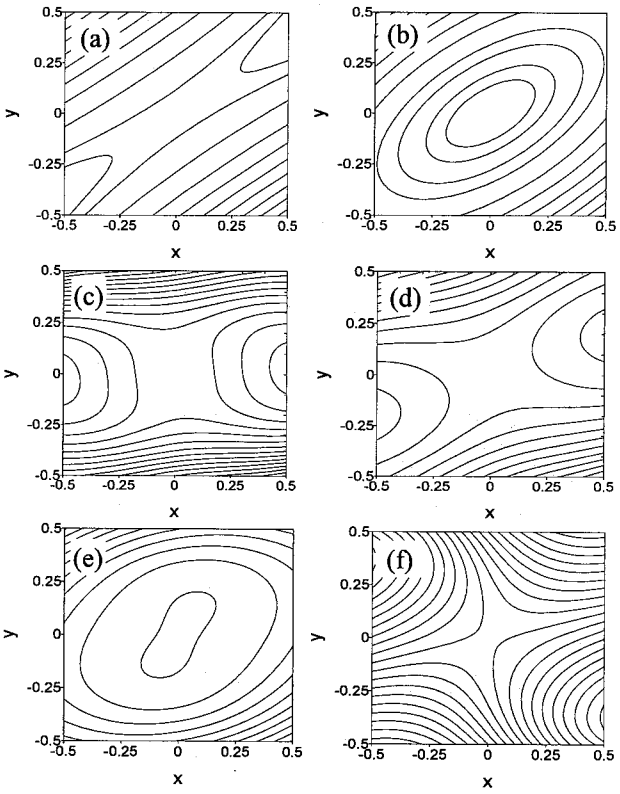

Fig.5 Turbulent structures by approximate solution for RUN-2: (a) k (b) ε (c) $\overline{u_1u_1}$ (d) $\overline{u_2u_2}$ (e) $\overline{u_3u_3}$ (f) $\overline{u_1u_2}$

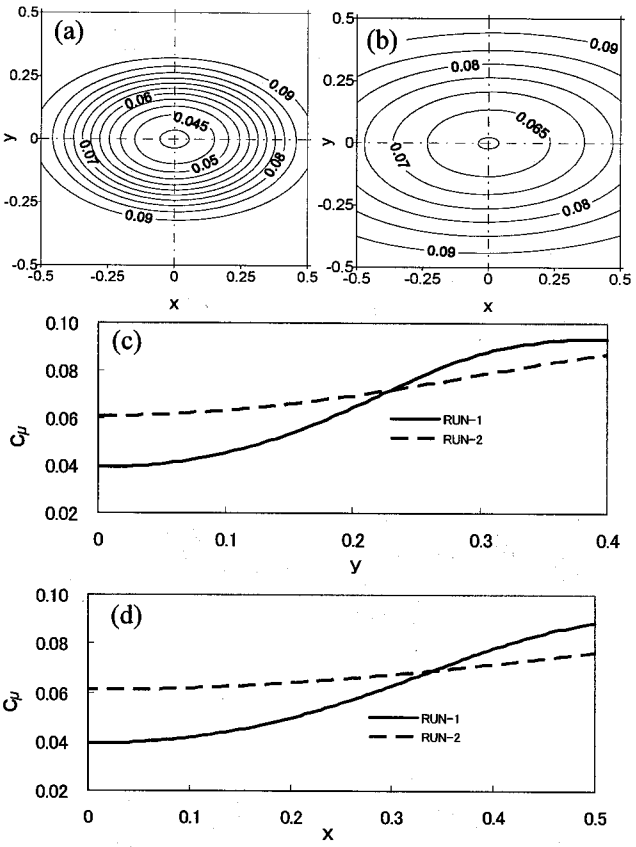

Fig.6 Distribution of c_μ in xy plane (a) RUN-1 (b) RUN-2; (c) c_μ profile along y-axis, (d) c_μ profile along x-axis [(0, 0) is the coordinate at vortex center].

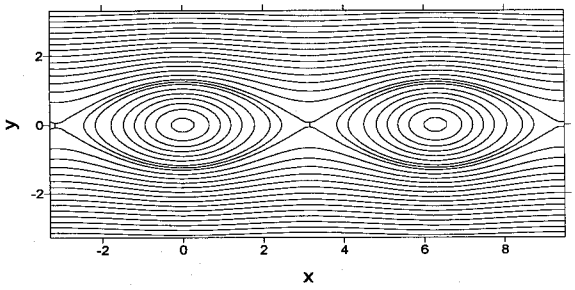

Fig.7 Streamlines of periodic Stuart vortices

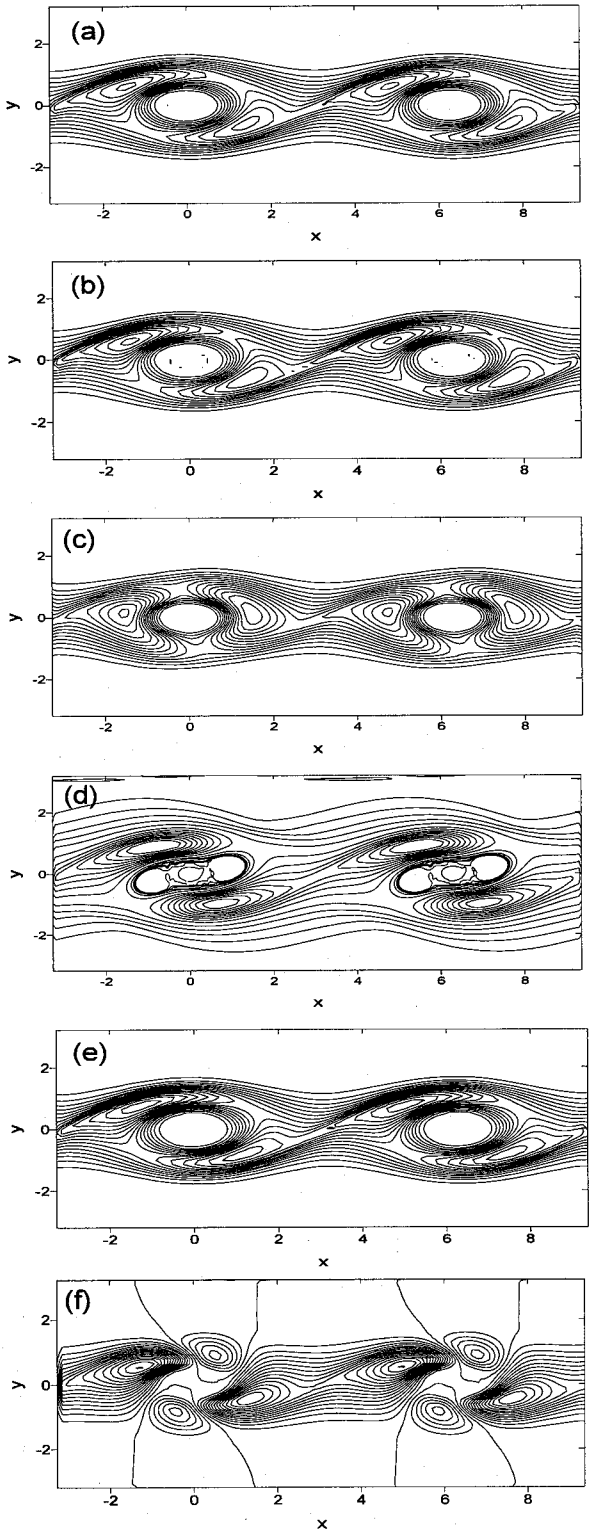

Fig.8 Turbulent structures by numerical simulation for RUN-1: (a) turbulent kinetic energy, k (b) turbulent energy dissipation rate, ε (c) turbulent normal stress in x direction, $\overline{u_1u_1}$ (d) turbulent normal stress in y direction, $\overline{u_2u_2}$ (e) turbulent normal stress in z direction, $\overline{u_3u_3}$ (f) turbulent shear stress in xy plane, $\overline{u_1u_2}$

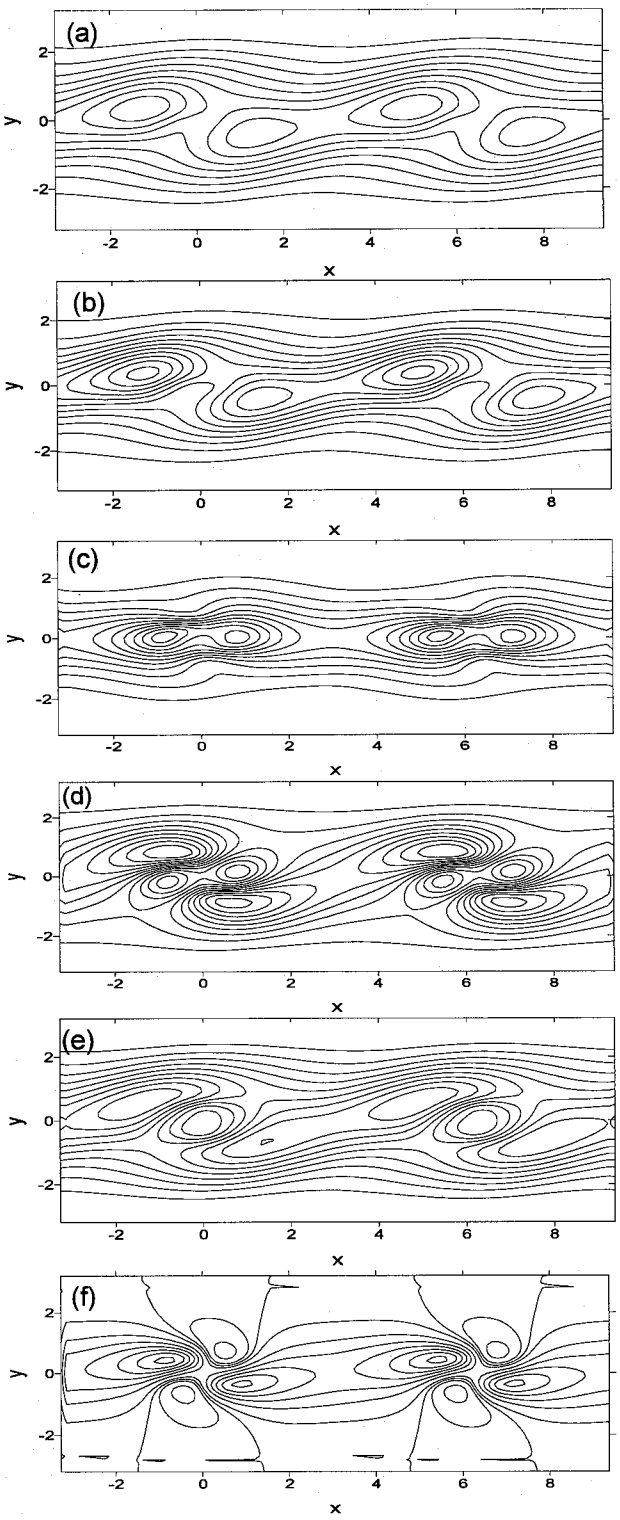

Fig.9 Turbulent structures by numerical simulation for RUN-2: (a) k (b) ε (c) $\overline{u_1u_1}$ (d) $\overline{u_2u_2}$ (e) $\overline{u_3u_3}$ (f) $\overline{u_1u_2}$

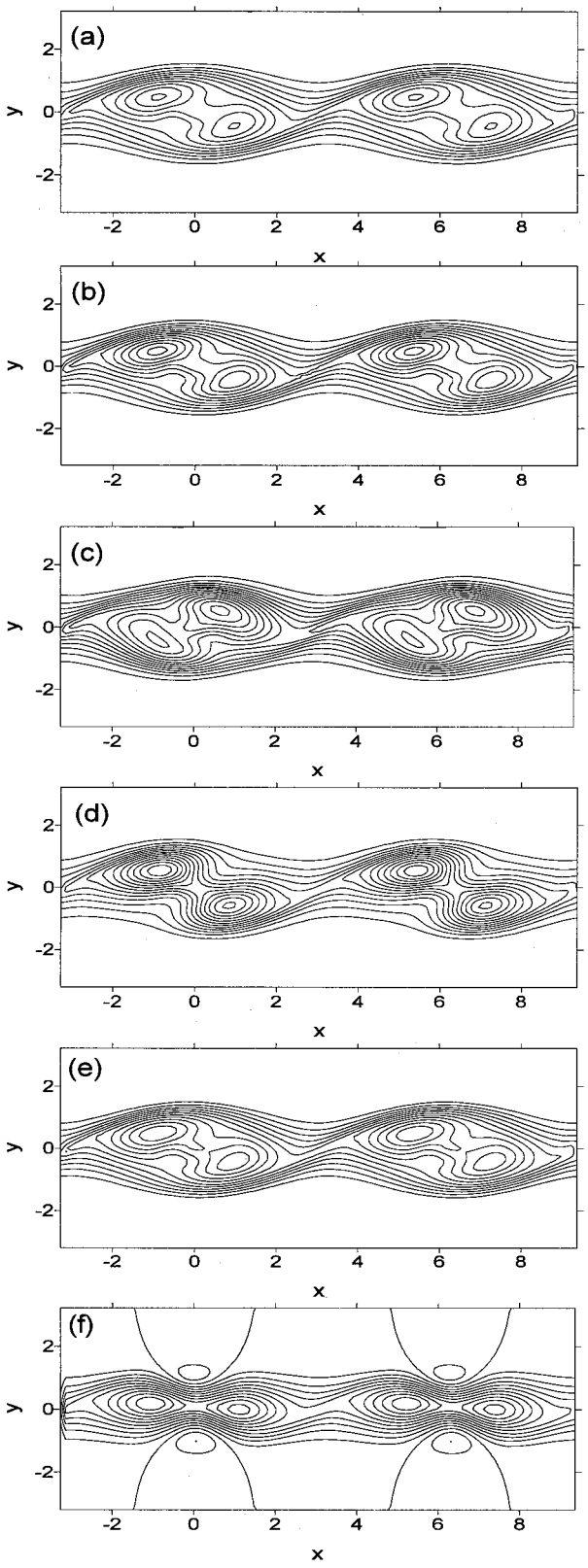

Fig.10 Turbulent structures by numerical simulation using Standard k-ε model: (a) k (b) ε (c) $\overline{u_1u_1}$ (d) $\overline{u_2u_2}$ (e) $\overline{u_3u_3}$ (f) $\overline{u_1u_2}$

Since, the values of RUN-1 predict the actual structures of the turbulent stresses (as per previous research[6]) near the focus of the vortex, it can be concluded that the present model with the estimated model constants is capable to simulate the flow field with large scale vortices.

5.2 Numerical simulation

In the previous section, approximate solutions are derived for the turbulent characteristics of Stuart vortices, and the model constants are estimated by tuning their values by numerous trials considering the turbulent structures. In this section, numerical simulations are carried out using the estimated model constants and the results are compared to approximate solution to assess the effectiveness of the approximate approach.

The equation of actual Stuart vortex expressed in Eq. (20) gives the following velocity field.

$$U_x = \frac{\partial \psi}{\partial y} = \frac{\sinh y}{\cosh y + A\cos x} \tag{40}$$

$$U_y = -\frac{\partial \psi}{\partial x} = \frac{A\sin x}{\cosh y + A\cos x} \tag{41}$$

For this velocity field, the turbulent stresses as well as k and ε profiles are determined. As shown in Fig. 7, two vortices are considered in the flow domain with a periodic boundary condition at upstream and downstream end.

The periodic turbulent structures simulated for RUN-1 are shown in Fig. 8. Turbulent kinetic energy (k) and its dissipation rate (ε), turbulent normal stress in x, y and z direction (expressed as $\overline{u_1u_1}$, $\overline{u_2u_2}$ and $\overline{u_3u_3}$ respectively) are showing the contours in elliptical shape at the vortex center. On the other hand, the turbulent shear stress in xy plane ($\overline{u_1u_2}$) is showing hyperbolic profile (saddle pattern). The results satisfy the approximate solution, and prove that the conditions derived for the constitutive law with the estimated model constants are applicable to simulate large scale vortices.

In the approximate solution it is shown that, the turbulent structure is changed with the change of the values of model constants; the evidence is also presented using the model constants of RUN-2. The simulation results for RUN-2 are presented in Fig. 9. Considering turbulent kinetic energy and turbulent normal stresses as shown in Fig. 9 (a), (c) and (d), the hyperbolic profiles (saddle pattern) are observed instead of elliptical one. The results of numerical simulation fully satisfy the approximate solution.

Fig. 6 shows that at the center of vortex, where the strain and rotation parameters are large, the value of c_μ is less than 1/2 of its far field value. However, in the standard k-ε model, the coefficient c_μ has no dependency on the rate of strain and rotation, and bears a constant value (=0.09) throughout the turbulent flow field. This deficiency of standard k-ε model causes an inconsistent prediction of turbulent structures at the center of vortex. Fig. 10 shows the results simulated by standard k-ε model. The model

failed to generate the elliptical profiles (focus pattern) for k, ε and turbulent normal stresses. The result is consistent with RUN-2 (Figs.5 and 9), where the value of c_μ is not sufficient to count the effect of strain and rotation rates.

From the consideration of spatial distribution, it is observed (RUN-1, Fig. 8) that the topological structures of turbulent normal stresses at vortex center are elliptic, and at saddle point the topology changes to hyperbolic profile (saddle pattern). The simulated results for turbulent structural topology in singular points are found compatible with that of previous experimental investigations of coherent structures in free shear flows[6].

6. Conclusion

Based on a realizable non-linear k– ε model, approximate solutions are derived for the turbulent properties of Stuart vortices. It is observed that the structures of turbulent stresses are changed with the values of constants. The values of model constants are tuned considering the predictability of turbulent structures near the vortex center; and the set of model constants that generates the actual structures of turbulent profiles, is considered to satisfy the necessary conditions for unsteady-RANS applicable to large-scale vortices.

The realizability conditions are also derived for a plane shear layer to estimate the constraints for the coefficients of eddy viscosity.

Numerical simulations are carried out using the estimated model constants and the results are compared to approximate solution to assess the effectiveness of the approximate approach. The results satisfy the approximate solution, and prove that the conditions derived for the constitutive law with the estimated model constants are applicable to simulate large scale vortices.

The topological structures of turbulent energy and it's dissipation as well as the turbulent intensities are found to be changed from elliptical to hyperbolic for the spatial change from vortex center to saddle point respectively.

Appendix: Notation of Symbols

$c_{\varepsilon 1}$, $c_{\varepsilon 2}$ = $k-\varepsilon$ model constants

c_μ, c_β (c_1, c_2, c_3) = non-linear $k-\varepsilon$ model constants

$c_{\mu 0}$, c_{ns}, $c_{n\Omega}$, c_{ds}, $c_{d\Omega}$, $c_{ds\Omega}$, c_{ds1}, $c_{d\Omega 1}$, $c_{ds\Omega 1}$ = model constants for c_μ

$c_{\beta 0}$ = the model constants for c_β

k = turbulent energy

k_{00}, k_{01}, k_{10}, k_{02}, k_{20}, k_{11}= coefficients of the assumed k distribution

m_{ds} , $m_{d\Omega}$ = model constants for c_β

P = pressure

S = strain parameter defined by Eq. (12)

S_{ij} = strain rate tensors

U_i = average velocity in x_i direction

U_x, U_y, U_z =velocities in Cartesian coordinate system

u_i = turbulent velocity in x_i direction

$\overline{u_i u_j}$ = Reynolds stress tensor

x_i =spatial coordinates

x, y, z = Longitudinal (stream-wise), transverse (width- wise), and vertical (depth-wise) directions in Cartesian coordinate system

ε = turbulent energy dissipation rate

ε_{00}, ε_{01}, ε_{10}, ε_{02}, ε_{20}, ε_{11} = coefficients of the assumed ε distribution

ρ = density of fluid

ν = molecular kinematic viscosity

ν_t = eddy viscosity

σ_k, σ_ε = $k-\varepsilon$ model constants

Ω = rotation parameter defined by Eq. (12)

Ω_{ij} = rotation rate tensor

References

1) Ali, M. S., Hosoda, T., Kimura, I., Onda, S., Approximate solution of an axisymmetric Swirling jet using non-linear k- ε model with consideration of realizability, *Journal of applied mechanics, JSCE* vol. 9, pp. 821-832, 2006

2) Yoshizawa, A., Statistical analysis of the deviation of the Reynolds stress from its eddy viscosity representation, *Phys. Fluids*, 27, pp.1377-1387, 1984.

3) Pope, S. B., A more general effective viscosity hypothesis, *J. Fluid Mech.* 72, pp.331-340, 1975.

4) Gatski, T. B. and Speziale, C. G., On explicit algebraic stress models for complex turbulent flows, *J. Fluid Mech.* 254, pp.59-78, 1993.

5) Kimura, I. and Hosoda, T., A non-linear k - ϵ model with realizability for prediction of flows around bluff bodies, *Int. J. Numer. Meth. Fluids.* 42, pp.813-837, 2003.

6) Hossain, A. K. M. F., Coherent structures and turbulence, *J. Fluid. Mech., 173*, pp. 303-356, 1986.

7) Rodi, W., Turbulence models for environmental problems, in *Prediction methods for turbulent flows (edited by W. Kollmann)*, pp.259, 1979.

8) Shih,T. H., Zhu, J. and Lumley, J. L., Calculation of bounded complex flows and free shear flows, *Int. J. Numer. Meth. Fluids.* 33, pp.1133-1144, 1996

9) Jaw, S.Y. and Chen, C. J., Present status of second order closure turbulence models. I: overview, *J. Engg. Mech., ASCE.* 124, pp.485-501, 1998.

(Received: April 13, 2007)